Mechanism of Associative Photoinduced Ligand Substitution in $W(CO)_4$phen under Metal-to-Ligand Charge-Transfer Excitation: Sub-Nanosecond Transient Spectra and Solvent and Wavelength Dependence Evidence for Rapid Primary Processes

Elspeth Lindsay, Antonín Vlček, Jr.,[†] and Cooper H. Langford*[,‡]

Canadian Centre for Picosecond Laser Spectroscopy, Concordia University, 1455 deMaisonneuve West, Montreal, Quebec, Canada H3G 1M8, and J. Heyrovský Institute of Physical Chemistry and Electrochemistry, Dolejškova 3, 18223 Prague, Czechoslovakia

Received February 3, 1993

Quantum yields for the photochemical reaction of $W(CO)_4$phen were evaluated under both ligand-field (LF) and metal-to-ligand charge-transfer (MLCT) excitation in a variety of conditions. Upon LF excitation, the quantum yield increased from 0.011 to 0.017 when the concentration of $(n\text{-Bu})_3P$ was increased from 0.015 to 0.36 M. This is interpreted as the indication of a minor associative pathway operating in competition with the known dissociative pathway. Excitation into different regions of the MLCT envelope revealed a complex wavelength and solvent dependence of the quantum yield. The quantum yield increases from 0.0024 to 0.0061 and from 0.0079 to 0.010 in solutions of $(n\text{-Bu})_3P$ in dichloromethane and tetrachloroethylene, respectively, on changing the irradiation wavelength from 488.0 to 514.5 nm. A similar wavelength change led to only a slight increase in quantum yield when the solvent was toluene. There was no demonstrable wavelength dependence in pyridine. This solvent dependence of the quantum yield is uncorrelated with the solvatochromism of MLCT bands. Excited-state absorption (ESA) was observed within 20 ps of excitation into either the LF (355-nm excitation) or the MLCT (532-nm excitation) band. Both the shape of the initial ESA envelopes and their evolution over time are distinguishably different upon change of excitation wavelength from 355 to 532 nm. The ESA is assigned to MLCT states of $W(CO)_4$phen (the ESA bands resembled the spectra of analogous one-electron-ligand-reduction products). These data imply the presence of two pathways for CO substitution, dissociative from the LF states and associative from the MLCT ones. Partition between these distinct pathways is controlled by early events which compete with the vibrational and electronic relaxation of the initial excited states. We suggest that two excited states, already distinguishable at 20 ps after excitation, include one which has relaxed in a way making it susceptible to nucleophilic attack.

Introduction

The compound $W(CO)_4$phen (phen = 1,10-phenanthroline) presents a special opportunity for explorations in photochemical theory. Ligand substitution processes occur from both a metal-to-ligand charge-transfer (MLCT) excited state and a ligand-field (LF) excited state, but by different pathways. Concentration and pressure dependence studies[1,2] have revealed that ligand substitution follows an associative mechanism upon irradiation into the MLCT band system. However, a dissociative pathway was observed upon excitation into the LF band.[1] Furthermore, multiple luminescence has been observed for many $W(CO)_4$-(α,α'-diimine) complexes, including $W(CO)_4$phen derivatives,[3] suggesting rather unusual photophysics in this family.

It is now clear that dissociation of CO following LF excitation commonly occurs promptly with time constants of the order of a vibration period[4-6] in $M(CO)_6$ complexes (M = Cr, W). Newly formed $W(CO)_5S$ and $Cr(CO)_5S$ (S = a solvent molecule) are "hot" and have vibrational relaxation times ≥15–20 ps on the ground-state potential surface.[5-9] These reactions in all probability involve excitation of specific vibrational degrees of freedom of the molecule as does the femtosecond stillbene isomerization recently described by Hochstrassser[10] and the initial step in the isomerization of rhodopsin[11] in which observation of products at 50 fs reveals breakdown of the Born–Oppenheimer approximation. We have been interested in such reactions for several years, using wavelength dependence over narrow spectral regions as diagnostic of chemical processes which compete with vibrational relaxation.[12]

In order to interpret what is occurring on such fast time scales, it is necessary to adopt an approach which is somewhat different from the "conventional" Born–Oppenheimer approximation. One approach which may help to identify the specifically excited vibrations considers that conservation of momentum involves a coupled response of all constituent electrons and nuclei. During the photochemically productive absorption, the translational and rotational momentum of the photochemically active photon is converted into internal motions of the molecule—not into its net translation or rotation. For this to be possible, the center of gravity and the axes of symmetry must remain unchanged, a condition realized only if all electronuclear accelerations from the photon event are compensated by opposing accelerations in the molecule. This requires that the molecule invoke all internal

[†] J. Heyrovský Institute.

[‡] Present address: Department of Chemistry, University of Calgary, 2500 University Dr., N.W., Calgary, Alberta, Canada T2N 1N4.

(1) Weiland, S.; Reddy, K. B.; van Eldik, R. *Organometallics* **1990**, *9*, 1802–1806.
(2) Van Dijk, H. K.; Servaas, P. C.; Stufkens, D. J.; Oskam, A. *Inorg. Chim. Acta* **1985**, *104*, 179.
(3) Rawlins, K. A.; Lees, A. J. *Inorg. Chem.* **1989**, *28*, 2154–2160.
(4) Langford, C. H.; Moralejo, C.; Sharma, D. K. *Inorg. Chim. Acta* **1987**, *126*, L11.
(5) Lee, M.; Harris, C. B. *J. Am. Chem. Soc.* **1989**, *111*, 8963.
(6) (a) Moralejo, C.; Langford, C. H.; Sharma, D. K. *Inorg. Chem.* **1989**, *28*, 2205. (b) Langford, C. H.; Moralejo, C.; Lindsay, E.; Sharma, D. K. *Coord. Chem. Rev.* **1991**, *111*, 337.
(7) (a) Joly, A. G.; Nelson, K. A. *Chem. Phys.* **1991**, *152*, 69. (b) Joly, A. G.; Nelson, K. A. *J. Phys. Chem.* **1989**, *93*, 2876.
(8) Moralejo, C.; Langford, C. H.; Sharma, D. K. *Inorg. Chem.* **1989**, *28*, 2205.
(9) Yu, S.; Xu, X.; Lingle, R.; Hopkins, J. B. *J. Am. Chem. Soc.* **1990**, *112*, 3668.
(10) (a) Repinec, S. T.; Sension, R. J.; Szarka, A. Z.; Hochstrasser, R. M. *J. Phys. Chem.* **1991**, *95*, 10380. (b) Sension, R. J.; Repinec, S. T.; Hochstrasser, R. M. *J. Chem. Phys.* **1990**, *93*, 9185.
(11) (a) Schoenlein, R. W.; Peteanu, L. A.; Mathies, R. A.; Shank, C. V. *Science (Washington, D.C.)* **1991**, *254*, 412. (b) Tallent, J. R.; Hyde, E. W.; Findsen, L. A.; Fox, G. C.; Birge, R. R. *J. Am. Chem. Soc.* **1992**, *114*, 1581.
(12) Langford, C. H. *Acc. Chem. Res.* **1984**, *17*, 96.

0020-1669/93/1332-2269$04.00/0

degrees of freedom in 3D space, requiring a complete description to have 2^3 distinct components. This leads to Hollebone's octupole selection rule:[13] $\Delta J + \Delta V = 3$ where ΔV is the change of a vibrational angular momentum quantum number and ΔJ is the change in electronic angular momentum (and is equal to $\Delta L + \Delta S$, where ΔS is the change in spin momenta and ΔL is the change in orbital momenta). Transitions into the ligand field bands have $\Delta V = 1$ or $\Delta V = 3$ and can show prompt dissociation because the response is an asymmetric bond stretch which can readily lead to rapid dissociation of the unique ligand. This approach has recently been successfully employed[6a] to explain excitation wavelength dependent photosubstitution of $W(CO)_5L$ (L = pyridine, piperidine) which occurs from a LF excited state.

Substitution reactions of MLCT states are mechanistically much less understood. According to the Hollebone selection rules, spin-allowed CT bands with electric dipole character have $\Delta L + \Delta S = 1$ (therefore, $\Delta V = 2$).[6] Thus, quadrupolar vibrations maintaining gerade structure (often detectable by Raman spectroscopy) will accompany allowed MLCT excitation. However, there is a low probability of driving a prompt dissociative response like those of $M(CO)_6$ because at least two atoms are put into motion to maintain gerade structure. This explains the common low reactivity toward substitution of MLCT states. On the other hand, relatively slow ($\tau \geq 1$ ns) photosubstitution from relaxed, long-lived MLCT states would provide an alternative explanation.

In order to elucidate some of these fundamental problems related to photosubstitutional reactivity of MLCT states of organometallics, we have focused on the primary processes of $W(CO)_4$phen upon irradiation into the MLCT and the LF bands. We combine results of sub-nanosecond spectroscopy and the wavelength and solvent dependence of the quantum yield upon excitation into the MLCT band. The concentration dependence of the quantum yield under LF excitation is also examined.

Experimental Section

Solvents. Unless otherwise specified, all solvents were of "spectrophotometric" grade. Acetonitrile, benzene, pyridine, toluene, dichloromethane, tetrachloroethylene, and tri-*n*-butylphosphine, $(n\text{-Bu})_3P$, were purchased from Aldrich and used as received. Tetrahydrofuran (THF) was obtained from BDH and was used without further purification except in the spectroelectrochemical measurements. The THF used in these experiments was purified by the ketyl method.

Materials. $W(CO)_4$phen was synthesized by refluxing $W(CO)_6$ (Aldrich, 99%) with excess 1,10-phenanthroline (Aldrich, 99+%) and trimethylamine *N*-oxide dihydrate (Aldrich, 98%) in acetonitrile (Aldrich, HPLC grade) for 1 h. Evaporation of the acetonitrile solution yielded crude $W(CO)_4$phen. The product was purified using column chromatography. A column of silica gel 60 (Baker reagent) was prepared using hexane (Baxter, HPLC grade) as the solvent. A 1:1 (v/v) mixture of hexane and dichloromethane (Caledon, spectrophotometric grade) and then neat dichloromethane were used to elute the product. The dichloromethane solution was then evaporated to dryness, affording pure $W(CO)_4$phen. The yield was 34%. The compound was characterized using UV–visible and infrared spectroscopy, which agreed with the spectra previously reported.[14] The extinction coefficients are 6040 and 3040 M^{-1} cm^{-1} for the MLCT band (486 nm) and the LF band (394 nm), respectively, in THF.

UV–Visible Spectroscopy. Conventional absorption spectra were recorded using a Hewlett-Packard Model No. 8452A diode array spectrophotometer interfaced with an IBM PC.

Spectroelectrochemistry. These experiments were conducted using apparatus previously described.[15] $W(CO)_4$phen was electrochemically reduced by one electron[16,17] to the corresponding anion, $[W(CO)_4phen]^-$. Absorption spectra were obtained spectroelectrochemically by a reduction of THF solutions containing 0.1 M $(n\text{-Bu})_4NPF_6$ on a Pt minigrind electrode in an optically transparent thin-layer (OTTLE) cell.[15]

Nanosecond Spectroscopy. Nanosecond spectroscopy was carried out under the auspices of Dr. D. J. Stufkens at the University of Amsterdam. The system has been previously described.[18] Nanosecond spectra were recorded using second-harmonic Nd/YAG excitation (532 nm) with pulse energies of either 20 or 40 mJ and a pulse width of approximately 10 ns and monitored with a 400–800-nm probe pulse. An OMA was used for data collection.

Picosecond Spectroscopy. Picosecond time-resolved spectroscopy was carried out with a system of conventional design and is described elsewhere.[6,19] Picosecond spectra following MLCT excitation were recorded using second-harmonic Nd/YAG excitation (532 nm) with a pulse energy of 2.5 mJ and a pulse width of approximately 30 ps. The diameter of the laser beam used to excite the sample was 1.5 mm. The probe pulse was derived from a fraction of the exciting pulse. This was focused onto D_2O to give a superbroadened probe covering the 425–675-nm range. A delay line enables the spectra to be recorded at delays from 0 ps to 10 ns after the exciting pulse. The changes in absorbance relative to the spectra obtained without excitation were recorded using an OMA. The spectra reported are the average of six to nine recordings. A similar procedure was used for excitation at 355 nm (third-harmonic Nd/YAG excitation); however the energy was intentionally limited to 1.2 mJ (at high pulse energy, there is some dc shift after 5 ns). Solutions of $W(CO)_4$phen used in these experiments were prepared under nitrogen in a Schlenk tube with an attached quartz cuvette (Hellma, 2-mm path length) and were thoroughly mixed between measurements. The absorbance at the exciting wavelength was between 0.3 and 0.5.

Steady-State Photochemistry. A PRA Model No. 3402 xenon medium-pressure arc lamp (150 W) coupled with an interference filter was used for photolysis at 365 nm. An argon ion laser (Coherent, 4 W—all line) was used for photolysis at 488.0 and 514.5 nm. For irradiation at 610.9 nm, a dye laser (Coherent CR-590) using Rh-6G was employed. The typical laser intensity incident on the sample was 120 mW (488.0, 514.5 nm) or 60 mW (610.9 nm). The beam was expanded to the diameter of the photolysis cell by passing it through a convex lens. Samples were prepared under an atmosphere of nitrogen in a Schlenk tube and then transferred (under nitrogen) to a quartz cuvette (Hellma, 1-cm path length, volume = 3.0 mL). Solution concentrations ranged from 9×10^{-4} to 1.5×10^{-3} M. In order to enhance the solubility of $W(CO)_4$phen in C_2Cl_4, 8% (v/v) CH_2Cl_2 was added to the solution. The concentration of $(n\text{-Bu})_3P$ was either 0.015, 0.30, 0.33, or 0.36 M. All solutions were stirred continuously during irradiation. All steady-state reactions were monitored by UV–visible absorption spectroscopy. The light intensity entering the photolysis cell at all wavelengths was determined using fulgide actinometry.[20] Quantum yields for the photoreactions were evaluated using the equations given in ref 21. Photoproduct extinction coefficients are required for these evaluations. They were obtained from the absorption spectra of the photoproduct measured after 100% photoconversion of the reactant. Isosbestic points were retained throughout the photolysis. The standard deviation for all measurements was less than 8%.

Results and Discussion

Electronic Spectroscopy. The electronic spectra of $W(CO)_4$phen in pyridine, dichloromethane, and toluene at 25 °C are shown in Figure 1. Negative solvatochromism of the low-lying band is observed, indicating CT character. This band has been assigned as a W → phen π^* CT transition in closely analogous $W(CO)_4$-(α,α'-diimine) complexes.[21,22] Servaas et al.[22a] have analyzed such MLCT band envelopes and assigned three MLCT transitions.

(13) Hollebone, B. R.; Langford, C. H.; Serpone, N. *Coord. Chem. Rev.* **1981**, *39*, 181.
(14) (a) Manuta, D. M.; Lees, A. J. *Inorg. Chem.* **1986**, *25*, 1354. (b) Balk, R. F.; Snoeck, T.; Stufkens, D. J.; Oskam, A. *Inorg. Chem.* **1980**, *19*, 3015.
(15) Krejčík, M.; Daněk, M.; Hartl, F. *J. Electroanal. Chem. Interfacial Electrochem.* **1991**, *317*, 179.
(16) Miholová, D.; Gaš, B.; Záliš, S.; Klíma, J.; Vlček, A. A. *J. Organomet. Chem.* **1987**, *330*, 75.
(17) Dessy, R. E.; Wieczorek, L. *J. Am. Chem. Soc.* **1969**, *91*, 4963.
(18) Martens, F. M.; Verhoeven, J. W.; Varma, C. A. G. O.; Bergwerf, P. *J. Photochem.* **1983**, *22*, 99.
(19) Moralejo, C. Ph.D. Thesis, Concordia University, Montreal, Canada, 1989.
(20) Heller, H. G.; Langan, J. R. *J. Chem. Soc., Perkin Trans. 2* **1981**, 341.
(21) Manuta, D. M.; Lees, A. J. *Inorg. Chem.* **1986**, *25*, 1354.
(22) (a) Servaas, P. C.; van Dijk, H. K.; Snoeck, T. L.; Stufkens, D. J.; Oskam, A. *Inorg. Chem.* **1985**, *24*, 4494. (b) Balk, R. W.; Stufkens, D. J.; Oskam, A. *Inorg. Chim. Acta* **1978**, *28*, 133.

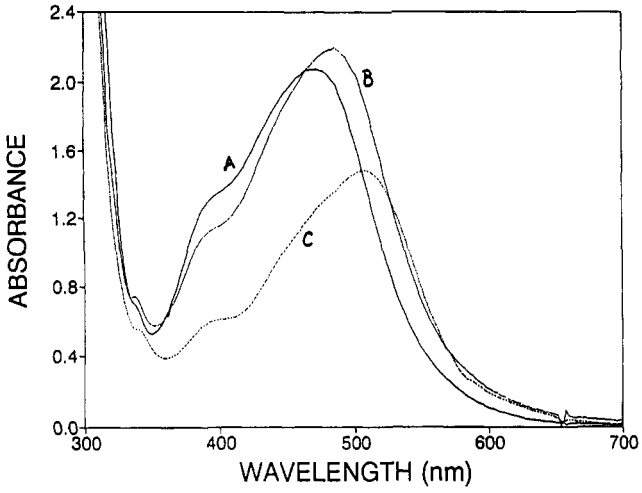

Figure 1. Electronic absorption spectra of 10^{-3} M W(CO)4phen in pyridine (A), dichloromethane (B), and toluene (C) at 293 K.

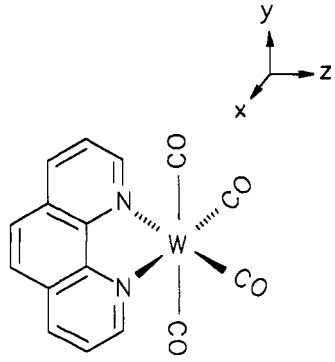

Figure 2. Representation of the W(CO)4phen molecule showing the coordinate system chosen.

The most intense transition is a z-polarized $(d_{yz})b_2 \rightarrow b_2(\pi^*)$ transition[22a] (refer to Figure 2 for the orientation of the axes of the W(CO)4phen molecule). We will refer to this intense low-energy system as MLCT⟨1⟩. The higher energy absorption at around 400 nm does *not* exhibit solvatochromism. It has been assigned as predominantly LF with a contribution from a higher energy $a_2 \rightarrow a_2(\pi^*)$ MLCT transition[3,21] which will be referred to as MLCT⟨2⟩. The band in the 300–350-nm region is also not solvatochromic, indicating LF character. These absorptions have been assigned to transitions to the two higher energy d_σ orbitals.[21]

Continuous Photolysis. The quantum yield of photochemical reactions whose mechanisms are uncomplicated by subsequent thermal processes is directly related to the quantum yields of the primary photochemical steps involved. Dependencies of quantum yields on reaction conditions (excitation wavelength, temperature, ligand concentration, ...) thus reveal detailed information on primary photochemical dynamics. Quantum yields of dissociative photosubstitution reactions are largely independent of the concentration of the substituting ligand. On the other hand, entering ligand concentration dependence of the quantum yield is a good diagnostic for an associative mechanism. Accordingly, quantum yields of the photosubstitution of W(CO)4(α,α′-diimine) complexes are concentration dependent upon MLCT excitation in the visible region of the spectrum.[1,2] Conversely, the substitution is known to follow a predominantly dissociative pathway under LF excitation.[1,2] In order to examine whether there is a contribution from the associative pathway even under LF excitation, dependence of the photosubstitution quantum yields of W(CO)4phen was measured as a function of the $(n\text{-Bu})_3P$ concentration in CH_2Cl_2 at 365 nm. (As may be seen in Figure 1, this excitation wavelength falls into the high-energy onset of the LF absorption band. The possibility of simultaneous excitation of both MLCT and LF transitions thus can clearly be neglected.)

Table I. Wavelength Dependence of the Quantum Yield[a] for the Photochemical Reaction of W(CO)4phen in Various Solvents[b]

wavelength (nm)	solvent	quantum yield[c]
365.0	neat pyridine	0.016(6.8)
	0.015 M $(n\text{-Bu})_3P$ in CH_2Cl_2	0.011(7.8)
	0.36 M $(n\text{-Bu})_3P$ in CH_2Cl_2	0.017(3.0)
488.0	neat pyridine	0.0028(4.1)
	0.3 M $(n\text{-Bu})_3P$ in toluene	0.0070(3.6)
	0.33 M $(n\text{-Bu})_3P$ in CH_2Cl_2	0.0024(2.9)
	0.3 M $(n\text{-Bu})_3P$ in C_2Cl_4	0.0079(2.1)
514.5	neat pyridine	0.0027(3.0)
	0.3 M $(n\text{-Bu})_3P$ in toluene	0.0079(5.8)
	0.36 M $(n\text{-Bu})_3P$ in CH_2Cl_2	0.0061(0.6)
	0.3 M $(n\text{-Bu})_3P$ in C_2Cl_4	0.010(4.4)
610.9	0.3 M $(n\text{-Bu})_3P$ in C_2Cl_4	0.028(4.0)

[a] All quantum yields were obtained at room temperature. [b] When C_2Cl_4 was the solvent, 8% (v/v) CH_2Cl_2 was added to the solution to enhance the solubility of W(CO)4phen. [c] The standard deviation (percent) is in parentheses.

From the results in Table I, it is evident that there is a concentration dependence under LF irradiation in CH_2Cl_2. The quantum yield increases from 0.011 to 0.017 upon increasing the concentration of $(n\text{-Bu})_3P$ in the reaction mixture from 0.015 to 0.36 M. This increase is comparable to that observed upon excitation into the MLCT band in the same solvent/ligand system, which suggests that the photosubstitution following LF excitation occurs by two mechanisms: a major dissociative reaction ($\Phi \simeq 0.01$) accompanied by a smaller ($\Phi \simeq 0.007$) contribution from an associative pathway. This observation clearly points to a population of MLCT state(s), even from LF state(s). This LF → MLCT conversion must therefore be an ultrafast process, kinetically competitive both with CO dissociation from the excited LF state(s) and with their relaxation to the ground state.

Dependence of the quantum yields on the excitation wavelength within the MLCT absorption band envelope was investigated in order to obtain more detailed insight into the reactivity of the MLCT states. Although the quantum yield observed upon MLCT excitation in neat pyridine remains unchanged (approximately 0.0028) with irradiation at 488.0 and 514.5 nm, the quantum yield is found to increase from 0.0024 (488.0-nm excitation) to 0.0061 (514.5-nm excitation) in solutions of 0.3 M $(n\text{-Bu})_3P$ in dichloromethane. Likewise, the quantum yield is found to increase from 0.0079 (488.0-nm excitation) to 0.010 (514.5-nm excitation) to 0.028 (610.9-nm excitation) in solutions of $(n\text{-Bu})_3P$ in tetrachloroethylene. However, the quantum yield only increases from 0.0070 (488.0-nm excitation) to 0.0079 (514.5-nm excitation) in a solution of 0.3 M $(n\text{-Bu})_3P$ in toluene. These results suggest that a significant increase in the quantum yield values with increasing excitation wavelength is typical for chlorinated solvents. There is a modest echo of this increase in toluene; however it is not observable in pyridine. The quantum yields increase with increasing wavelength of the MLCT absorption band maximum in the solvent series CH_2Cl_2 (λ_{max} = 486 nm), toluene (λ_{max} = 510 nm), and C_2Cl_4 (λ_{max} = 534 nm), if the nucleophile, $(n\text{-Bu})_3P$, and its concentration are kept constant. Due to the solvatochromism, the 488.0- and 514.5-nm excitation wavelengths fall on the low-energy side of the band in CH_2Cl_2, are close to the band maximum in toluene, and are to the high-energy side of the band in C_2Cl_4. The wavelength dependence thus points to higher reactivity upon excitation into the low-energy part of the MLCT band whereas the solvent dependence implies the opposite. It is therefore important to realize that there are separate but coupled wavelength and solvent dependencies upon excitation into various regions of the MLCT band envelope which do not correlate with the solvatochromism and are thus not attributable to changes in initial distribution of Franck–Condon excited-state population. This establishes the importance of events at very early times after excitation. It is known that the rates of vibrational relaxation are dependent on

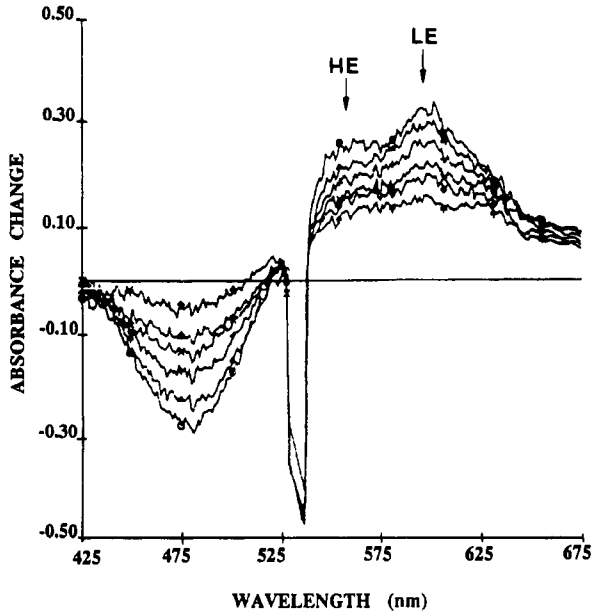

Figure 3. Transient absorption spectra of $W(CO)_4$phen in pyridine using 355-nm excitation recorded at probe delays of 50 and 500 ps and at 1, 2, and 5 ns in order of decreasing absorbance change. The arrows indicate the high-energy (HE) and the low-energy (LE) components of the ESA.

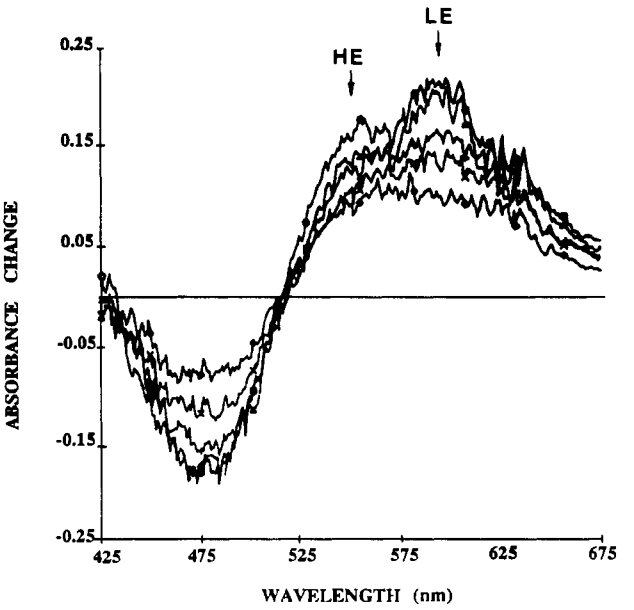

Figure 4. Transient absorption spectra of $W(CO)_4$phen in pyridine using 532-nm excitation recorded at probe delays of 50 and 500 ps and at 1, 1.5, 2, and 5 ns in order of decreasing absorbance change. The arrows indicate the high-energy (HE) and the low-energy (LE) components of the ESA.

thermal conductivity of the solvent medium.[23] Halogenated hydrocarbons have a lower thermal conductivity than the nonhalogenated hydrocarbons, slowing dissipation of excess vibrational energy and, hence, the relaxation into the reactive excited state. Both solvent and wavelength dependences clearly show that the partition between relaxation channels, one of them being the reactive one, must be decisively influenced by events occurring in competition with vibrational relaxation. The molecule must "decide" which pathway it will follow within the few-picosecond time domain of vibrational relaxation[23] following the initial MLCT excitation.

Transient Absorption Spectroscopy. Transient absorption spectra of $W(CO)_4$phen were recorded using LF (355 nm) and MLCT (532 nm) excitation in both polar and nonpolar solvents and using both nanosecond and picosecond pulses. The nanosecond spectra obtained between 400 and 800 nm with 532-nm excitation indicate the presence of a transient (band maximum at approximately 580 nm in acetonitrile) that is formed within the pulse and decays completely in 8 ns. This work made clear that no excited-state absorption (ESA) of lifetime longer than 8 ns is important and that the bands observed between 425 and 650 nm are the only significant ESA bands. Therefore, we present only the picosecond spectra in detail. Representative ESA spectra in pyridine are shown in Figure 3 (355-nm excitation) and Figure 4 (532-nm excitation). Inspection of the transient absorption spectra show that the transients are fully developed in less than 20 ps under both 355- and 532-nm excitation. They decay subsequently. Spectra obtained in other solvents showed similar behavior. Numerical results are summarized in Tables II and III. There are three characteristic features which can be found in each spectrum. In all, the ground-state band is bleached within 20 ps and recovers subsequently. Two decaying ESA features are identified by a "higher energy", HE, and a "lower energy", LE, band maximum which decay within approximately 1 ns (Tables II and III) to yield a longer lived residual absorption at 5 ns, but nanosecond spectroscopy shows it decays shortly thereafter.

The general features of the ESA spectra under both 355- and 532-nm excitation are similar. However, quantitative examination reveals unequivocally that the initial (20 ps) contributions of the higher energy and the lower energy band maxima vary with excitation wavelength and solvent (this is most reliably demonstrated by calculation of the ratio of the peak value absorbance change at 20 ps to the depth of the absorbance change minimum where the ground state is bleached; this eliminates any effects of variation in the pulse energy). The two components (higher and lower energy) decay with distinguishable solvent-dependent rates. Thus, it is clear that ESA is observed for two distinct excited states which are both fully formed at 20 ps and which are formed in different ratios under different irradiation wavelengths. Again, we see evidence for a decisive influence of early events prior to 20 ps.

In all cases, bleach recovery follows biexponential kinetics, the faster component being comparable with the decay rate constant of the transient absorption (see Tables II and III). As in the ESA, there is a longer-lived component of the bleached ground-state absorption that is still present at 5 ns. The observed ESA extends into the blue region, over the same area as the bleach (475 nm). This is concluded because the absorbance change for the bleach (475 nm) is approximately –0.3 whereas the ground-

Table II. Data for Picosecond Flash Phototransients of $W(CO)_4$phen[a] in Various Solvents (λ_{pump} = 355 nm)

	solvent		
	acetonitrile[b]	pyridine	benzene[c]
τ (ns) (HE[d] ESA)	1.1 ± 0.1	1.0 ± 0.1	*e*
τ (ns) (LE[d] ESA)	0.7 ± 0.1	2.0 ± 0.1	1.6 ± 0.2
τ (ns) (bleach)	3.6 ± 0.8	1.8 ± 0.1	0.9 ± 0.1
ground-state	452 ± 2	472 ± 2	508 ± 2
band max (nm)	390 (sh) ± 2	390 (sh) ± 2	390 (sh) ± 2
bleach (nm)	452 ± 10	480 ± 10	495 ± 10
HE ESA (nm)	538 ± 10	550 ± 10	*e*
LE ESA (nm)	582 ± 10	590 ± 10	584 ± 10
dielectric constant[f]	35.95	12.01	2.28

[a] All transient absorption spectra were obtained at room temperature. [b] To enhance the solubility of $W(CO)_4$phen in acetonitrile, 0.02 M H_2O was added to the reaction mixture. [c] To enhance the solubility of $W(CO)_4$phen in benzene, 0.05 M pyridine was added to the reaction mixture. [d] HE and LE refer to the high-energy and the low-energy components of the ESA, respectively. [e] The ESA blue-shifted (with respect to what was observed in the other solvents) and no HE component was observed when benzene was the solvent. [f] Data were obtained from: *Nonaqueous Electrolyte Handbook*; Janz, Tomkins, Eds.; Academic Press, Inc.: New York, 1972; Vol. 1.

(23) Elsaesser, T.; Kaiser, W. *Annu. Rev. Phys. Chem.* **1991**, *42*, 83.

Table III. Data for Picosecond Flash Photolysis on $W(CO)_4$phen[a] in Various Solvents (λ_{pump} = 532 nm)

	solvent		
	acetonitrile	pyridine	benzene
τ (ns) (HE[b] ESA)	0.4 ± 0.1	1.1 ± 0.1	*c*
τ (ns) (LE[b] ESA)	1.0 ± 0.2	1.2 ± 0.2	1.2 ± 0.2
τ (ns) (bleach)	1.8 ± 0.2	1.3 ± 0.1	1.3 ± 0.2
ground-state band max (nm)	452 ± 2	472 ± 2	508 ± 2
	390 (sh) ± 2	390 (sh) ± 2	390 (sh) ± 2
bleach (nm)	460 ± 10	479 ± 10	495 ± 10
HE ESA (nm)	560 ± 10	560 ± 10	*c*
LE ESA (nm)	587 ± 10	596 ± 10	597 ± 10
dielectric constant[c]	35.95	12.01	2.28

[a] All transient absorption spectra were obtained at room temperature. [b] HE and LE refer to high-energy and low-energy components of the ESA, respectively. [c] The ESA blue-shifted (with respect to what was observed in the other two solvents) and no high-energy ESA was observed when benzene was the solvent. [d] Data were obtained from: *Nonaqueous Electrolyte Handbook*; Janz, Tomkins, Eds.; Academic Press, Inc.: New York, 1972; Vol. 1.

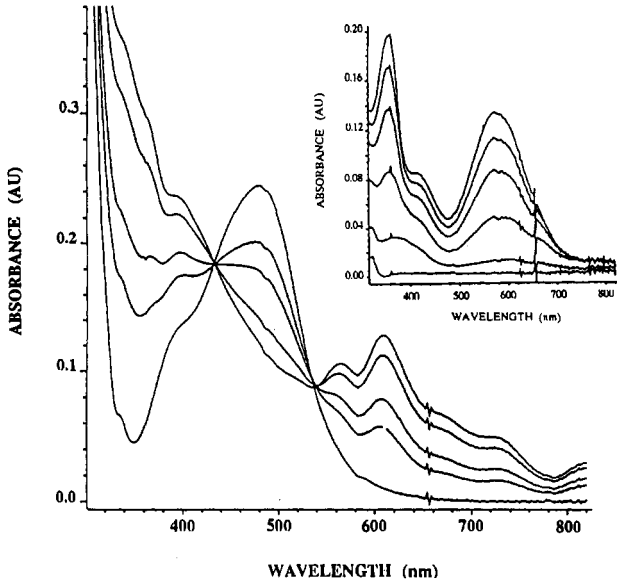

Figure 5. Spectroelectrochemical reaction of $W(CO)_4$phen in THF solution containing 0.1 M $(n\text{-Bu})_4NPF_6$. The spectra displayed in the inset show the reduction of the free phen ligand.

state spectrum has an absorbance of 0.9 at 475 nm when pyridine is the solvent.

Assignment of ESA. The low overall quantum yields for substitution allow us to eliminate the possibility that primary photoproducts account for the transients observed at 20 ps. Because the quantum yield is so low under both LF and MLCT excitation, it is not expected that a solvato species, a possible precursor to the photoproduct, will give an observable transient. Further evidence that the transient absorption is not due to the solvato species is the observation that very similar transients are formed in both coordinating (THF, CH_3CN, pyridine) and noncoordinating (CH_2Cl_2, benzene) solvents. Only a very small negative solvatochromism is observed in the transient absorption spectra. It is unlikely that a LF excited state would show any noticeable solvatochromism whereas a ligand-localized electron in a MLCT state is likely to interact with the solvent, leading to some solvatochromism in its further excitation. We therefore assign the transients as MLCT states. More direct evidence for this assignment is obtained from the results of spectroelectrochemical experiments (Figure 5). The spectrum of the reduced $[W(CO)_4phen]^-$ complex is very similar to the spectrum of the uncoordinated radical anion of the ligand ($phen^-$) (Figure 5, inset), indicating that the extra electron is ligand-localized in the reduced complexes which thus can be formulated as a $W(CO)_4(phen^-)$ species. Additionally, these bands are of similar shape and in the

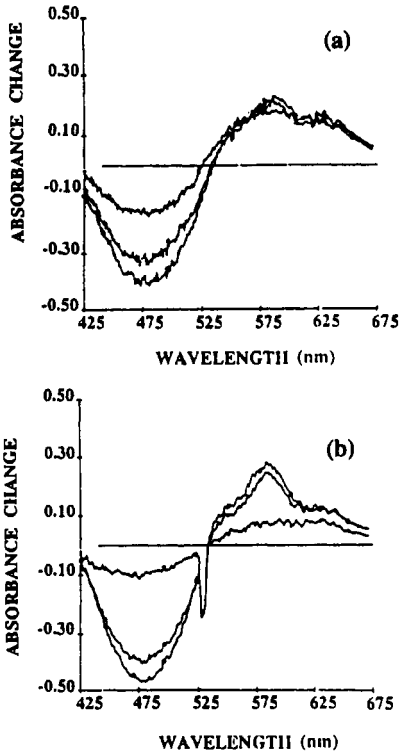

Figure 6. Transient absorption spectra of $W(CO)_4$phen in THF using (a) 355-nm and (b) 532-nm excitation recorded at probe delays of 50 and 500 ps and at 5 ns in order of decreasing absorbance change.

same region as the ESA for $W(CO)_4$phen in the same solvent (Figure 6), thus lending further support to the assignment of the transients as MLCT states which may be viewed as $[W^I(CO)_4(phen^-)]$. Hence, the ESA is assigned as an essentially $\pi \rightarrow \pi^*$ transition of the reduced $phen^-$ ligand found in MLCT-excited $W(CO)_4$phen. Analogous qualitative correspondence between the ESA spectrum of a MLCT excited state and a spectrum of a one-electron-reduced species was observed[24] for $Ru(bipy)_3^{2+}$. Overall, the observed transient is most likely a combination of a short-lived MLCT state (the sharper peak on the low-energy side of the transient absorption which rapidly decays; τ = 1.1 ns) and another longer lived MLCT excited state (the broad band which decays in about 8 ns, as observed in the nanosecond spectra). Most probably, these states are members of the MLCT⟨1⟩ manifold whose presence was inferred[3] from emission spectra of the closely related $W(CO)_4$(4-Me-phen) complex. According to this emission study,[3] such individual ^{3}MLCT states are less than 1000 cm^{-1} apart. This energy difference is comparable with that between the short-lived (~1 ns) and long-lived (~5 ns) ESA transients. The observed excited-state dynamics occurring between 20 ps and 5 ns may then be viewed as an equilibration[3] of the ^{3}MLCT⟨1⟩ excited-state manifold.

Observation of ESA due to MLCT states even after excitation at 355 nm indicates that those LF excited states which do not undergo CO dissociation (fraction >0.98) can relax to a ^{3}MLCT state or states. This LF → MLCT conversion efficiently competes with the CO dissociation from the LF states, limiting the quantum yield observed at 355 nm to about 0.01. This interpretation of the transient absorption spectra fully agrees with the presence of a minor associative photochemical pathway in addition to the dissociative pathway which operates upon LF excitation as was established by the quantum yield measurements. Note that the states reached promptly, i.e. in competition with the subpicosecond CO dissociation from the LF state, are identical to those generated by 532-nm MLCT excitation. If CO dissociation

(24) Braterman, P. S.; Harriman, A.; Heath, G. A.; Yellowlees, L. J. *J. Chem. Soc., Dalton Trans.* **1983**, 1801.

is a sub-picosecond process,[7] it would seem that LF → ^{3}MLCT conversion is similarly rapid.

A Model for the Associative Photochemistry. The prompt appearance of the ESA (<20 ps) and the similarity in coordinating and noncoordinating solvents suggest that the events initiating the associative pathway (i.e. formation of the reactive MLCT state) occur on the same short time scale as those controlling CO dissociation from the LF state. This idea is strongly reinforced by the observed wavelength dependence. In this context, the response of the steady-state yield to changes of nucleophile does not suggest prompt formation of a 7-coordinate species incorporating the entering ligand. In neat pyridine, where all complexes excited are in encounter with a ligand, the observed yield is smaller than that for 0.3 M phosphine, where it is unlikely (from the Fuoss–Eigen equation[25]) that more than 20% of the complexes are in encounter with a phosphine molecule at the time of excitation (and in the first nanosecond after). Thus, our first suggestion is that *the associative pathway involves bimolecular attack by a nucleophile on a suitable vibrationally relaxed excited state* (or possibly a relaxed intermediate).

In pyridine, where all excited states are in encounter with the nucleophile, the kinetics of attack reduce to first order. If we assume that nucleophilic attack and relaxation to the ground state are competing paths of the excited state, the quantum yield of ~0.003 implies an attack rate constant of about 3×10^6 s^{-1} if the reaction is with an excited state which decays at about 1×10^9 s^{-1} (if the longer lived state is assumed to be the reactive one, the rate constant would be 1 order of magnitude smaller). The corresponding phosphine rate constant is about 2×10^7 s^{-1} if the encounter equilibrium constant is predicted by the Fuoss–Eigen equation. Thus, the associative pathway appears to arise in two stages. First, an excited state (or primary intermediate) which is susceptible to facile nucleophilic attack is formed rapidly (<20 ps). After this step, the species relaxes and reacts with nucleophiles in competition with its nanosecond relaxation back to the ground state. Beyond this statement lies speculation, but some of the speculation is useful in illustrating clearly how the system acquires sensitivity to nucleophilic attack which is at least 10 orders of magnitude greater than the susceptibility of the ground state. After all, the remarkable accelerations which some pathways experience in excited states have not often been given concrete explanation and even first steps in this direction may fruitfully suggest new experimentation.

Staal et al. have shown, using resonance Raman (rR) spectroscopy,[26] that the $Mo(CO)_4$ moiety in $Mo(CO)_4$(*i*-Pr-DAB) (*i*-Pr-DAB = $C_{10}H_{16}N_2$) changes from C_{2v} microsymmetry to C_{4v} microsymmetry upon cooling. Clearly, the distortion is not blocked by a high barrier. If it is true that an excited $W(CO)_4$phen can also undergo a distortion, this excited state can become more favorable for attack by a nucleophile on the W atom to form a capped octahedron, a 7-coordinate species. The rate constants calculated in the last section require a specific MLCT species lacking a high barrier to nucleophilic attack. Two other important factors contribute to the reduction of the barrier for all of the MLCT states. First, the MLCT state has W in the 1+ formal oxidation state.[27] As well, the configuration at the metal is d^5, not d^6. Both should considerably facilitate nucleophilic attack. These are general factors, and the conformational effect or some similar mechanism must select the particular state responsible for reaction.

Associative vs Dissociative Pathway. The presence of two different photosubstitution pathways raises the important question of why differences between the photochemistry of the LF and MLCT states should arise in these prompt processes. Since we argue that key events determining the relative efficiency of the partition between the associative, dissociative, and nonreactive relaxation pathways are very fast steps in the domain of breakdown of the Born–Oppenheimer approximation,[10,11] it is interesting to see whether the Hollebone octupole selection rule can provide an explanation for the dissociative reaction from a LF state and associative reaction from a MLCT state. The Hollebone selection rules offer an approach in the spirit of Woodward–Hoffmann or Longuet–Higgins–Abrahamson rules.

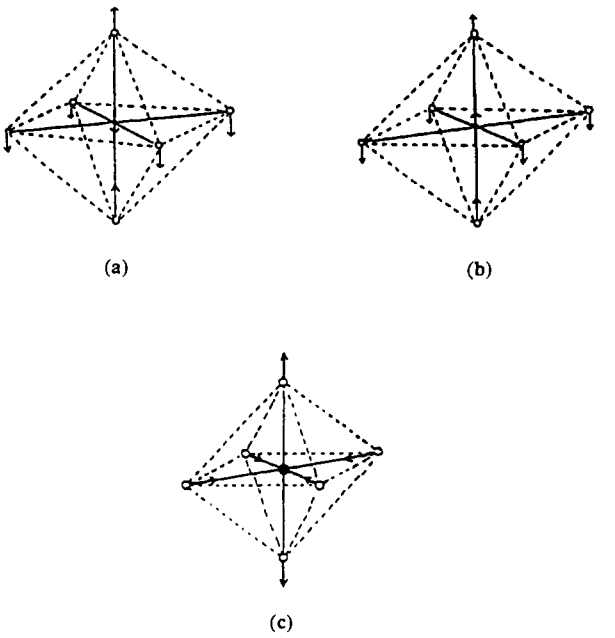

Figure 7. Simplified diagrams representing (a) the asymmetric stretch mode of a t_{1u} vibration, (b) the buckle mode of a t_{1u} vibration, and (c) the ν_2 mode of vibration in O_h.

Symmetry selection rules for prompt relaxation have been introduced by Hollebone et al.[13] which indicate the preferred nuclear coordinate connecting two electronic states if overall angular momentum is to be conserved in the vibronic process. This theory is based on subduction from spherical symmetry to a lower symmetry (O_h or C_{2v}). In octahedral symmetry, the requirements of the point group imply coupling of LF (d–d, gerade transitions) with two types of t_{1u} vibrations. The one associated with $\Delta V = 1$ is the asymmetric stretch (Figure 7a) and that associated with $\Delta V = 3$ is the "buckle" (Figure 7b). If we apply the octupole rule to a d^6 complex such as $W(CO)_4$phen, approximated as an O_h system, the LF transitions are

transition	ΔL	ΔS	ΔV	(O_h)
$^1T_1(I) \longleftarrow {}^1A_1(I)$	0	0	3	t_{1u} buckle
$^3T_1(P) \longleftarrow {}^3A_1(I)$	1	1	1	t_{1u} stretch

The vibration associated with the triplet excited state and corresponding to $\Delta V = 1$ is the asymmetric stretch (Figure 7a). In this mode, there is substantial extension along one axis; hence the ligand on that axis should be susceptible to substitution via a square pyramid intermediate. The singlet excited state ($\Delta V = 3$) is associated with a buckling mode of vibration, as shown in Figure 7b. This mode is expected to be very reactive toward substitution via a nonselective path because the metal is highly exposed to solvating molecules on four octahedral faces above the x,y plane. Such variation in selectivity has been observed in $W(CO)_5L$ (L = pyridine, piperidine).[28] Hence, loss of CO is expected upon excitation into the singlet LF state. If the time scale of the dissociation is fast, as in the case of $W(CO)_6$,

(25) Shriver, D. F.; Atkins, P. W.; Langford, C. H. In *Inorganic Chemistry*; Oxford University Press: Oxford, U.K., 1990; p 479.
(26) Staal, L. H.; Terpstra, A.; Stufkens, D. J. *Inorg. Chim. Acta* **1974**, *34*, 97.
(27) Perng, J. H.; Zink, J. *Inorg. Chem.* **1990**, *29*, 1158.
(28) Moralejo, C.; Langford, C. H. *J. Photochem. Photobiol., A* **1991**, *59*, 285.

dissociation of a CO molecule is the most likely consequence of 355-nm irradiation.

Spin-allowed CT bands with electric dipole character[6] have $\Delta V = 2$. The vibration associated with a $\Delta V = 2$ is the ν_2 mode in octahedral geometry (Figure 7c). This ν_2 mode reflects the requirement to put at least two atoms into motion to maintain gerade structure. Although, there is low probability of prompt dissociative response, the main consequence of such a vibration is an opening of the faces of the octahedron, a plausible prerequisite for the formation of a 7-coordinated associative intermediate. This implies the presence of two distinct reaction pathways for the reaction of $W(CO)_4$phen. The observation of a dissociative pathway upon excitation into the LF singlet is predicted by the excitation of $\Delta V = 1$ or 3 t_{1u} vibrations. An associative pathway upon MLCT irradiation is consistent with the prediction of excitation of a $\Delta V = 2$ vibration, leading to a *conformational rearrangement* which makes the molecule more susceptible to nucleophilic attack. The Hollebone rules have given fruitful insight into three d^6 systems ($W(CO)_4$phen, $W(CO)_5L$ (L = piperidine, pyridine),[6,19,28] and the complex[29] $Co(NH_3)_5X^{2+}$). It remains a matter of considerable interest to see how widespread are the predictive successes.

Acknowledgment. We thank the Natural Sciences and Engineering Research Council of Canada for support of this work. We also thank Andries Terpstra (Universiteit van Amsterdam) for recording the nanosecond spectra and Dr. František Hartl (J. Heyrovský Intitute) for the spectroelectrochemical measurements. E.I. acknowledges the hospitality of the Anorganisch Chemisch Laboratorium, Universiteit van Amsterdam, during a visit. Prof. Derk J. Stufkens, our collaborator in a number of investigations, was generous with his advice and council. This work could not have been brought to fruition without his assistance. As usual, work in the Canadian Centre for Picosecond Laser Spectroscopy has depended on the expert guidance of the director, Dr. D. K. Sharma.

(29) Malkhasian, A. Y. S.; Langford, C. H. *J. Am. Chem. Soc.* **1987**, *109*, 2682.